

***Electronic Supplementary Information
prepared for Dalton Transactions***

Address correspondence to:

Seiji Ogo, Professor
International Institute for Carbon–Neutral Energy Research
(WPI-I2CNER), Kyushu University
744 Moto–oka, Nishi–ku, Fukuoka
819–0395, Japan
Phone: 81-92-802-2818
Fax: 81-92-802-2823
E-mail: ogotcm@mail.cstm.kyushu-u.ac.jp

**A model for the water-oxidation and recovery systems
of the oxygen-evolving complex**

A table of contents

Fig. S1	page S1
Fig. S2	page S2
Fig. S3	page S3
Fig. S4	page S4
Fig. S5	page S5
Fig. S6	page S6
Fig. S7	page S7
Fig. S8	page S8
Fig. S9	page S9
Fig. S10	page S10
Fig. S11	page S11
Fig. S12	page S12
Fig. S13	page S13
Fig. S14	page S14
Fig. S15	page S15
Fig. S16	page S16

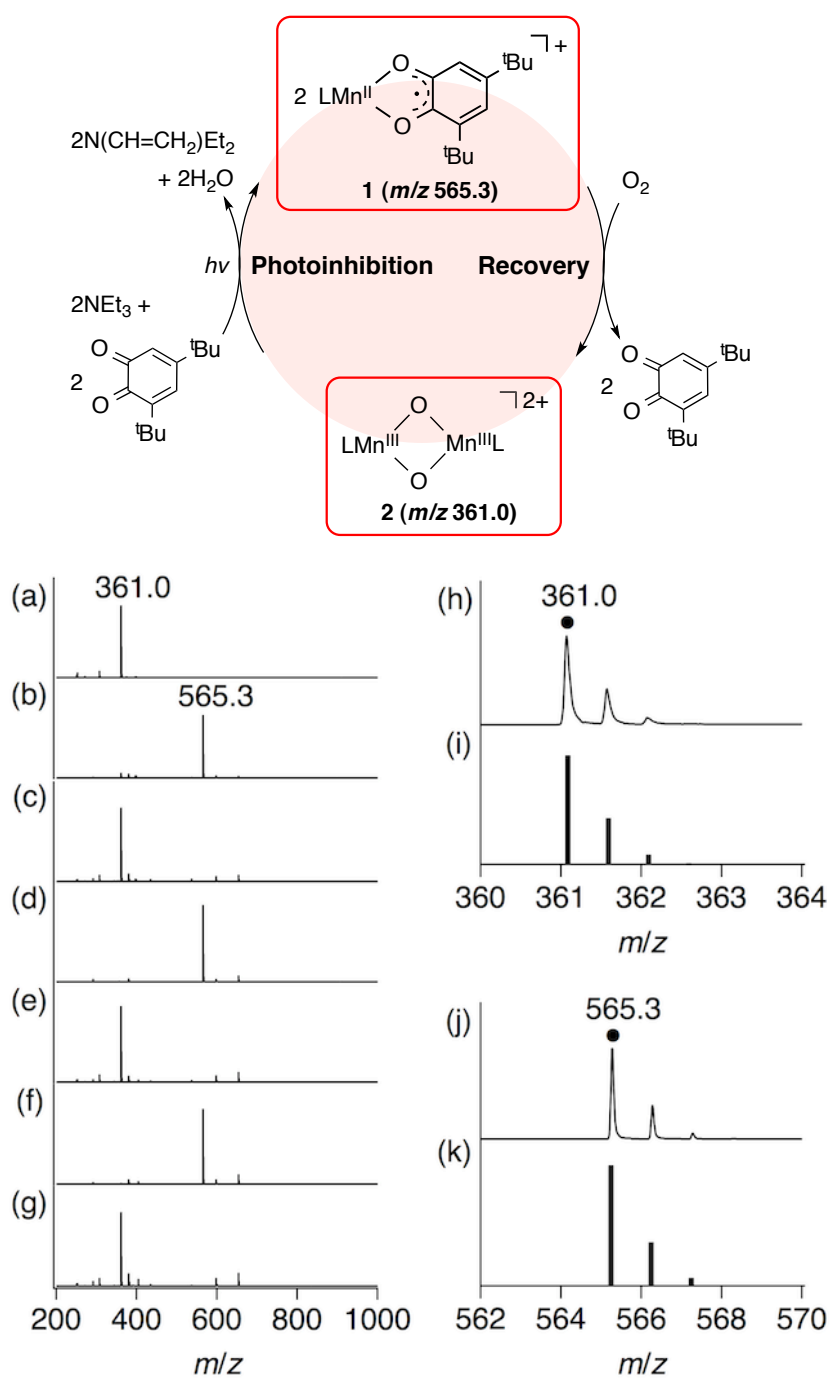


Fig. S1 Positive-ion ESI mass spectral change for the repeated cycle of photoreduction of **2** and oxygenation of **1**. The spectra of **1** shown in (b), (d) and (f) were obtained from photo-irradiation of **2** shown in (a), (c) and (e), respectively. The spectra of **2** shown in (c), (e) and (g) were obtained from oxygenation of **1** shown in (b), (d) and (f), respectively. (h) The signal at m/z 361.0 corresponds to $[\mathbf{2}]^{2+}$. (i) Calculated isotopic distribution for $[\mathbf{2}]^{2+}$. (j) The signal at m/z 565.3 corresponds to $[\mathbf{1}]^+$. (k) Calculated isotopic distribution for $[\mathbf{1}]^+$.

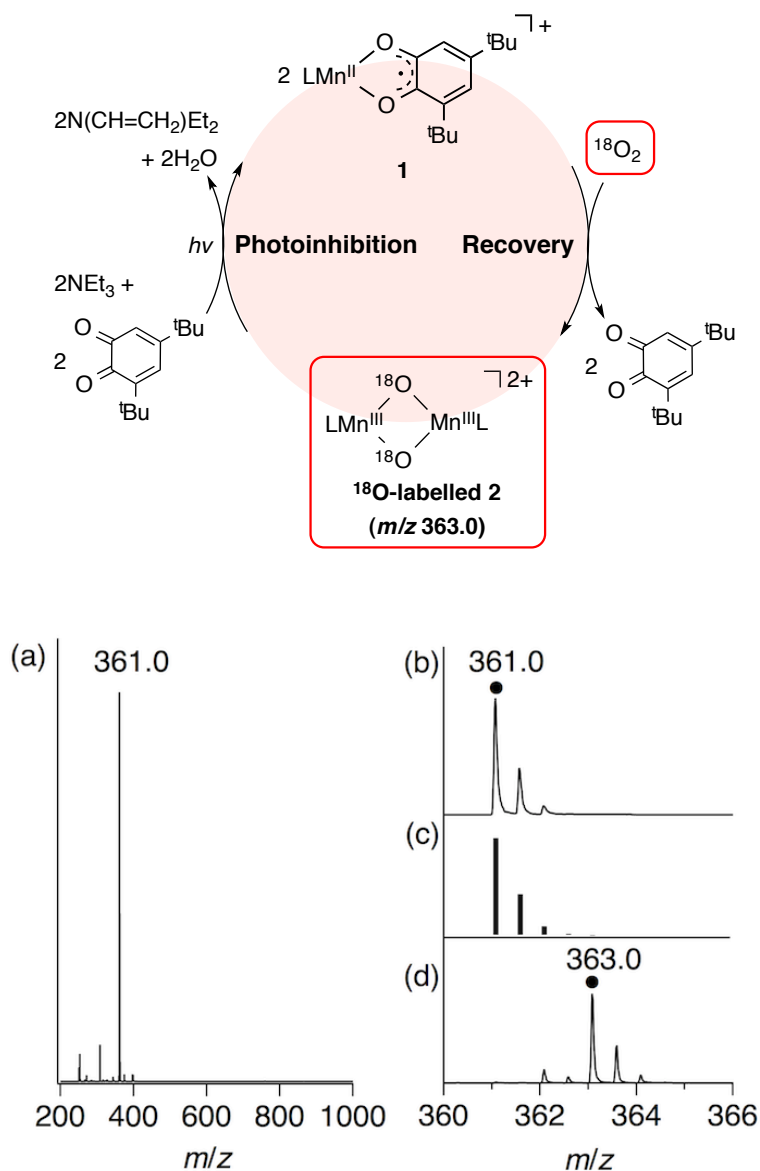


Fig. S2 (a) Positive-ion ESI mass spectrum of **2** in CH_3CN , which is obtained from the photo-irradiation of **2** and successive oxygenation of **1**. (b) The signal at m/z 361.0 corresponds to $[\mathbf{2}]^{2+}$. (c) Calculated isotopic distribution for $[\mathbf{2}]^{2+}$. (d) Positive-ion ESI mass spectrum of $[\text{Mn}^{\text{III,III}}_2(\text{TPA})_2(\mu\text{-}^{18}\text{O})_2]^{2+}$ (^{18}O -labelled **2**) in CH_3CN , which is obtained from the photo-irradiation of **2** and successive oxygenation of **1** using $^{18}\text{O}_2$. (b) The signal at m/z 363.0 corresponds to $[\text{}^{18}\text{O}\text{-labelled } \mathbf{2}]^{2+}$.

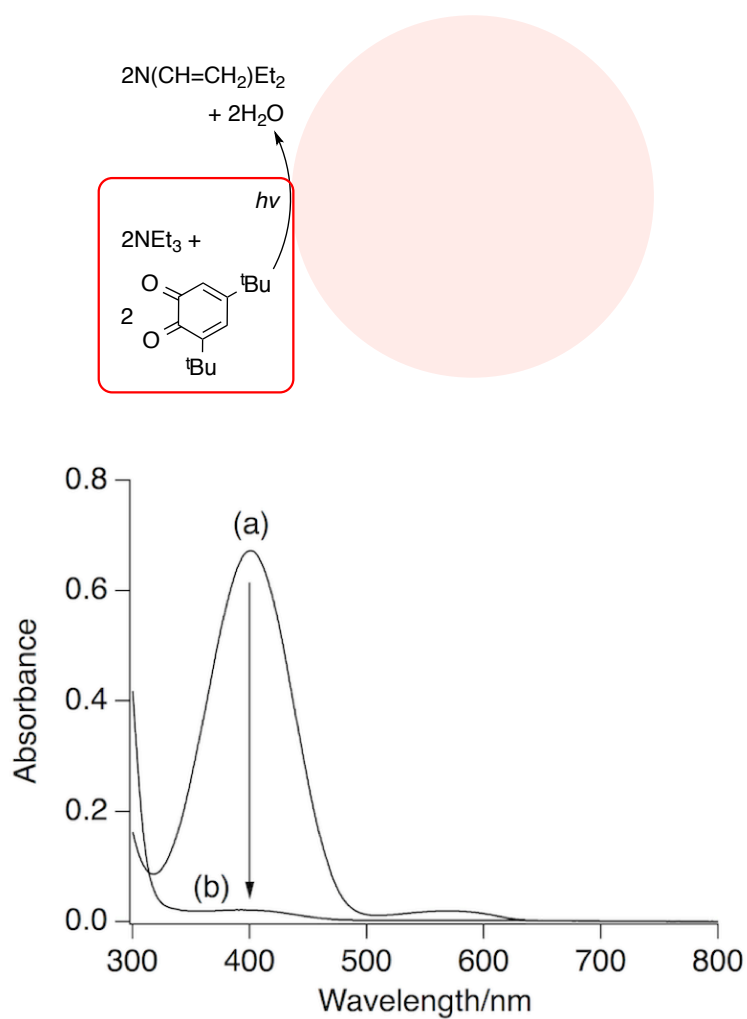


Fig. S3 UV-vis spectra of 3,5-di-*t*-butyl-1,2-benzoquinone (DTBBQ) (400 μM) and NEt_3 (4.0 mM) in CH_3CN (2.5 mL) (a) before and (b) after photo-irradiation (>550 nm).

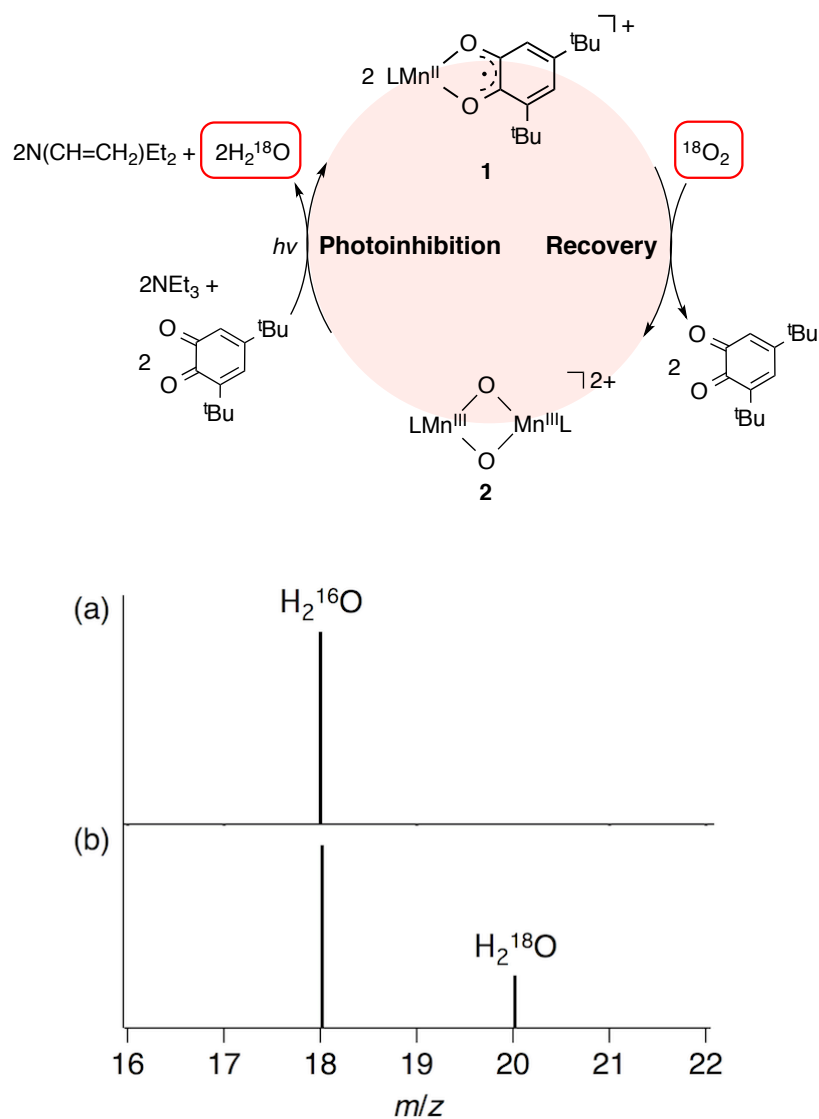


Fig. S4 Positive-ion GC-mass spectra of H₂¹⁶O and H₂¹⁸O obtained from the reaction of **2** (1.4 mg, 1.0 μmol) with (a) ¹⁶O₂ (5.0 mL) and (b) ¹⁸O₂ (5.0 mL) in the presence of 3,5-di-*t*-butyl-1,2-benzoquinone (DTBBQ) (22 mg, 100 μmol) and NEt₃ (140 μL, 1.0 mmol) in CH₃CN (200 μL) under photo-irradiation (>550 nm).

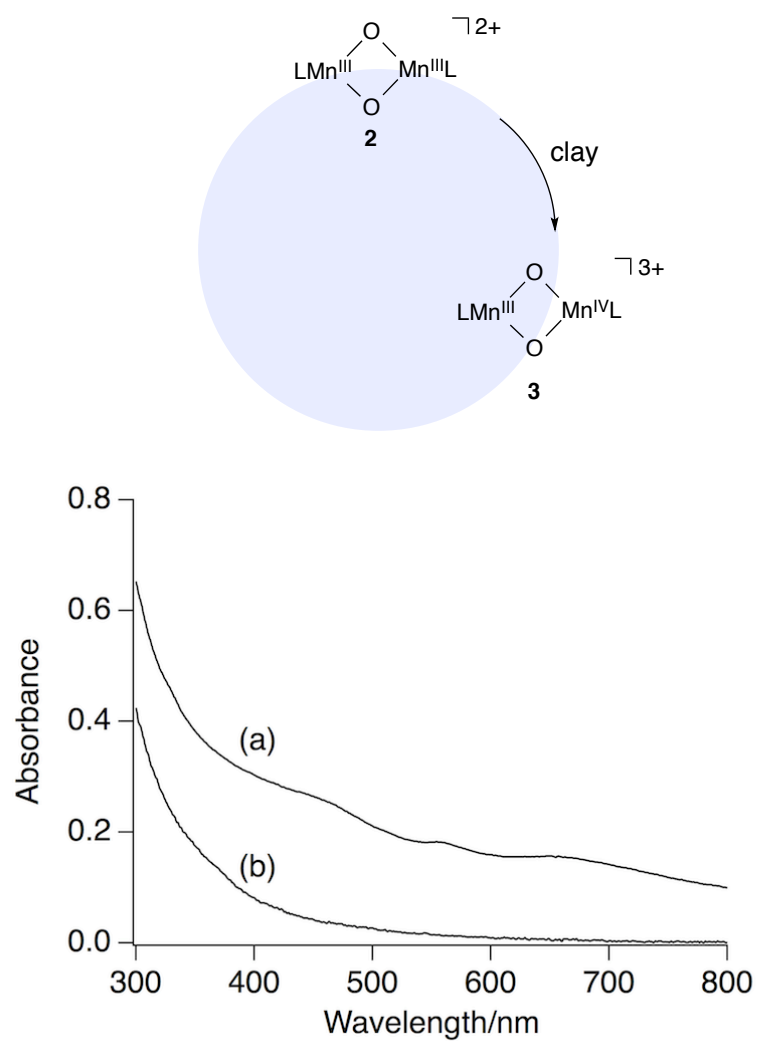


Fig. S5 Diffuse reflectance UV-vis spectra of (a) 2·3@Clay and (b) clay.

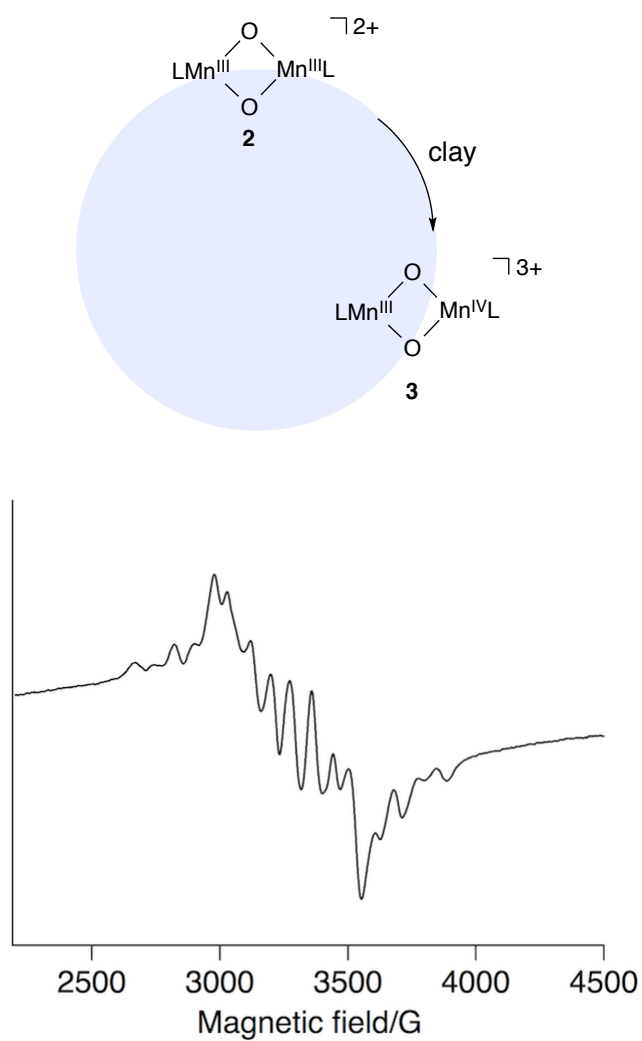


Fig. S6 ESR spectrum of **2·3@Clay** (5.0 mg, content of the mixture of **2** and **3**: 300 nmol) suspended in DMF (500 μ L) at -150 °C (microwave frequency: 9.16 GHz, microwave power: 1.0 mW).

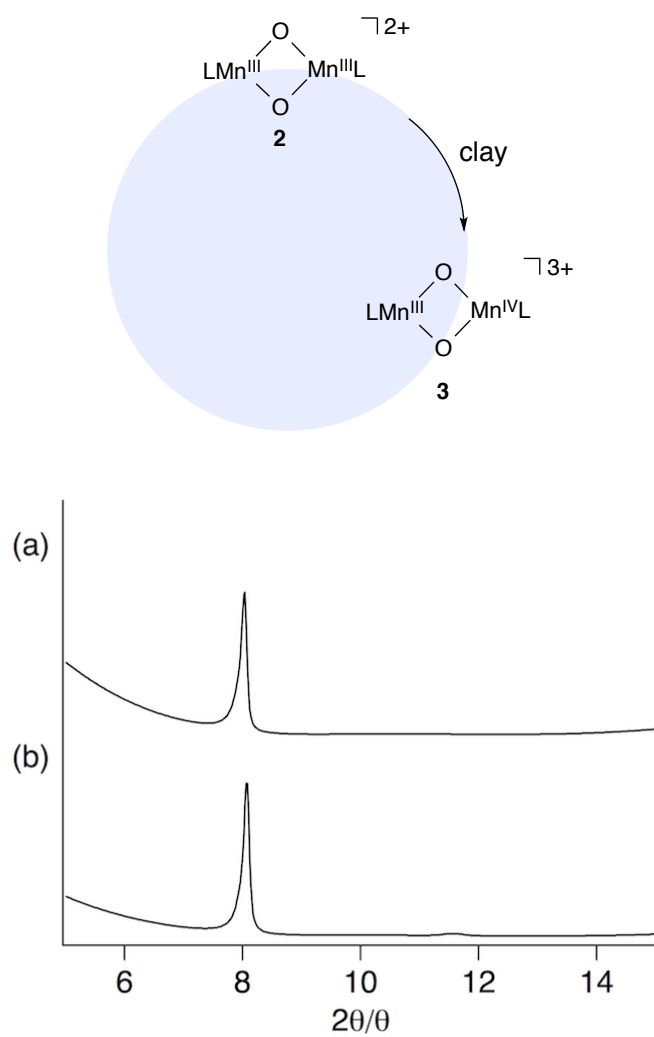


Fig. S7 XRD patterns of (a) **2·3@Clay** and (b) clay.

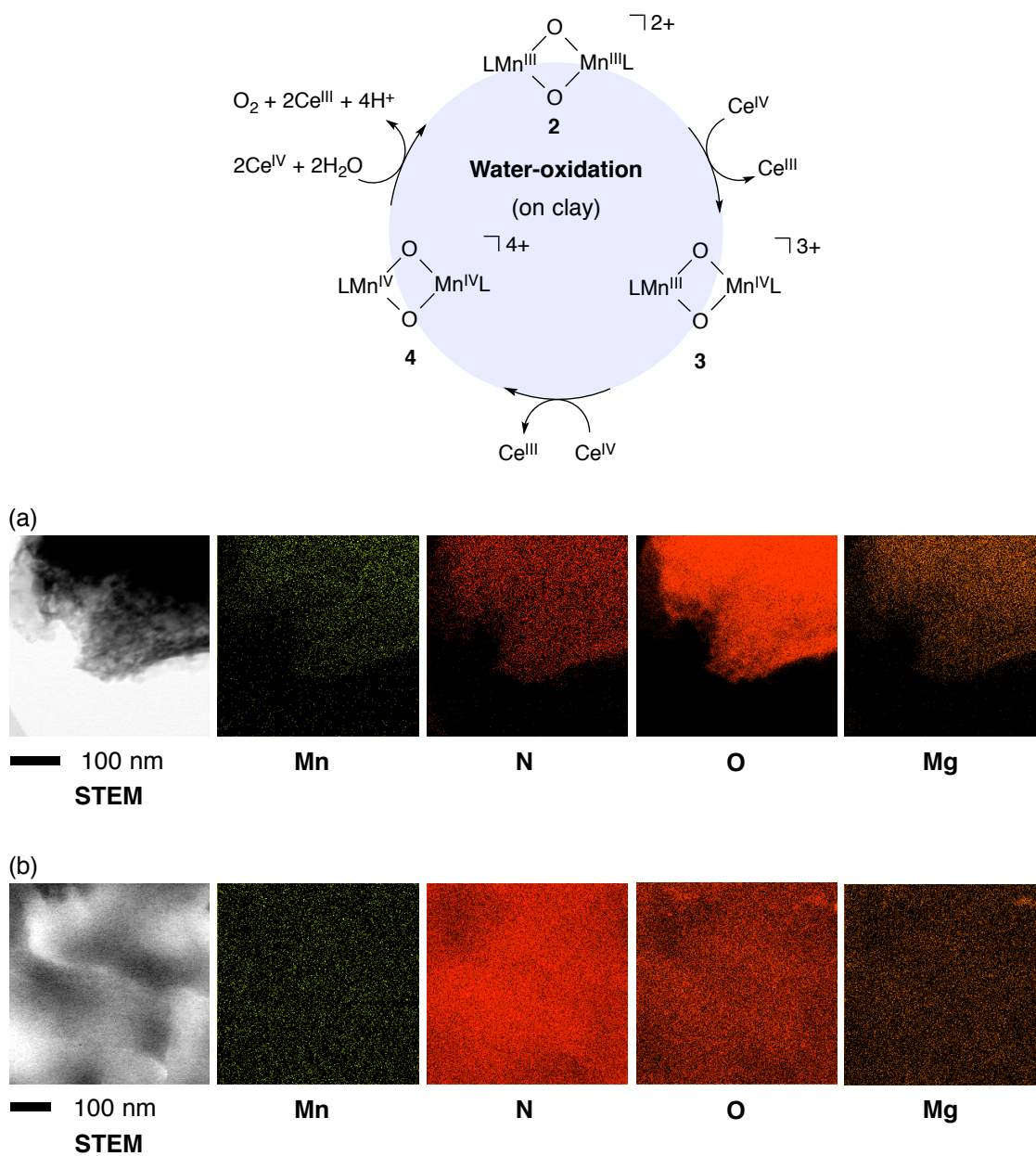


Fig. S8 STEM images and EDS elemental mappings of (a) **2·3@Clay** and (b) clay material isolated from the mixture of **2·3@Clay** and Ce^{IV} .

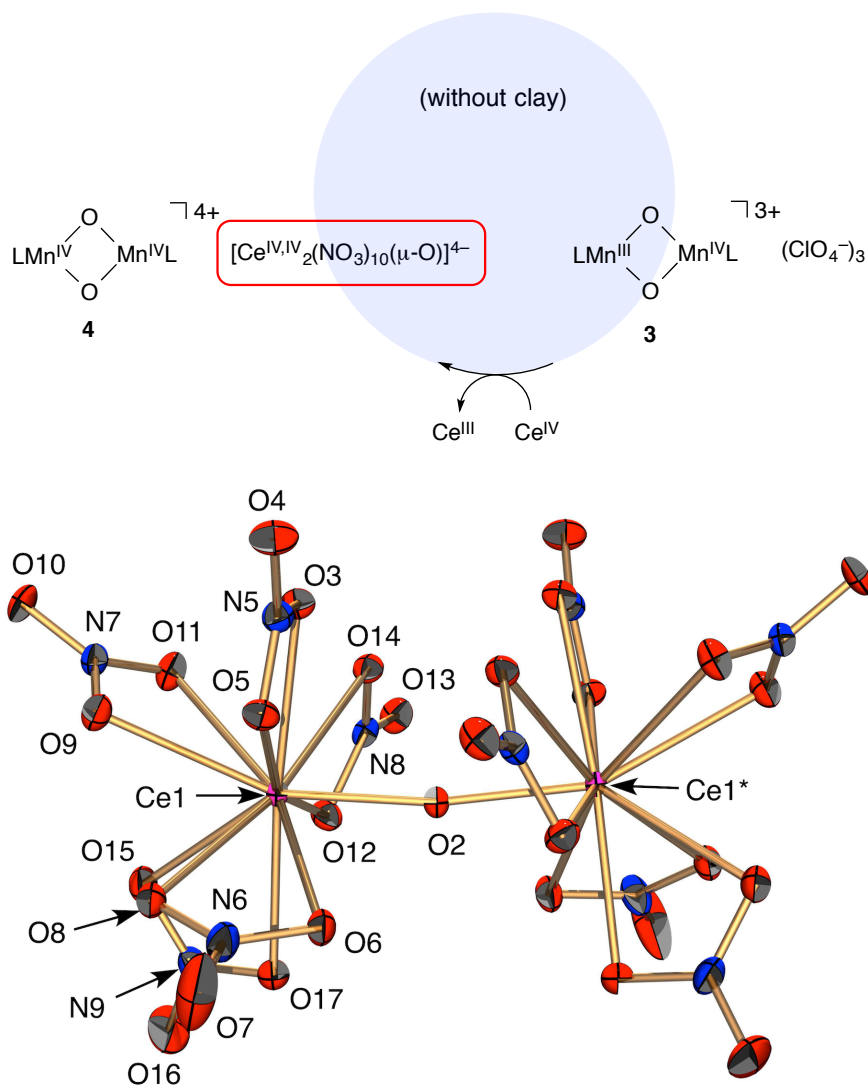


Fig. S9 ORTEP drawing of $[\text{Ce}^{\text{IV,IV}}_2(\text{NO}_3)_{10}(\mu\text{-O})]^{4-}$ with ellipsoids at 50% probability. The counter cation $[\text{Mn}^{\text{IV,IV}}_2(\text{TPA})_2(\mu\text{-O})_2]^{4+}$ (**4**) is omitted for clarity. Selected interatomic distance (\AA) and angle ($^\circ$): $\text{Ce1-O2} = 2.0480(2)$, $\text{Ce1-O2-Ce1}^* = 170.70(11)$.

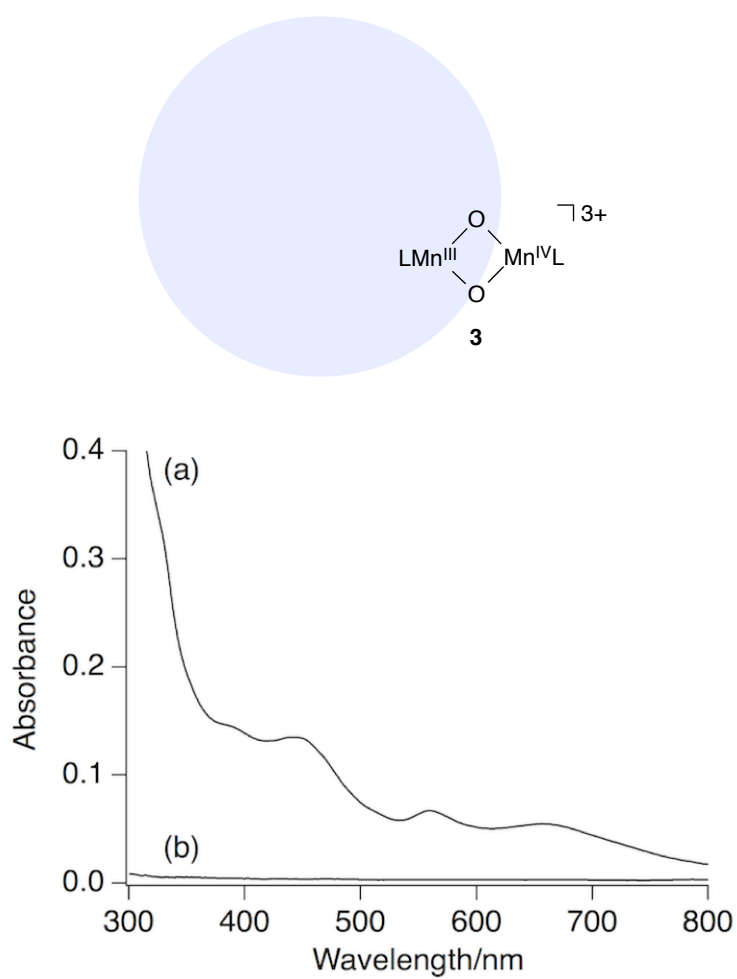


Fig. S10 UV-vis spectra of (a) the CH₃CN solution of **3** (100 μM) and (b) the supernatant CH₃CN/water solution after adsorption of **3** on clay.

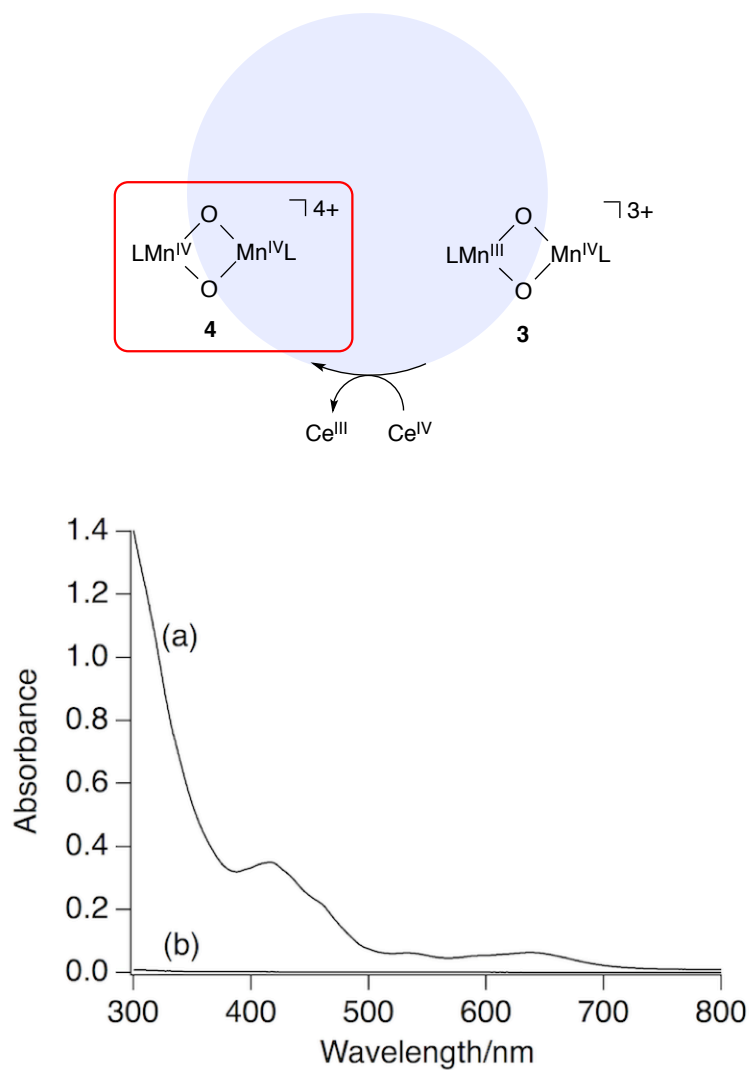


Fig. S11 UV-vis spectra of (a) the aqueous solution of **4** (1.0 mM) and (b) the supernatant aqueous solution after adsorption of **4** on clay.

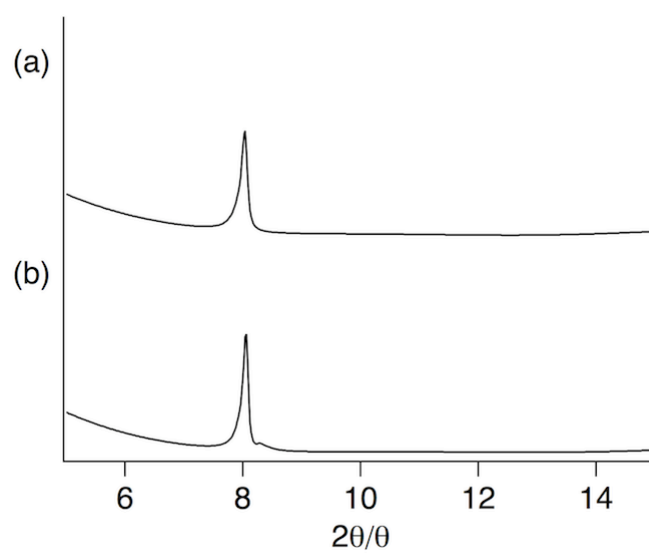
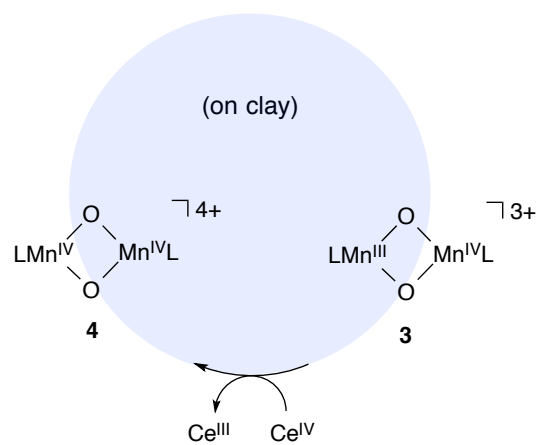


Fig. S12 XRD patterns of (a) $3@Clay$ and (b) $4@Clay$.

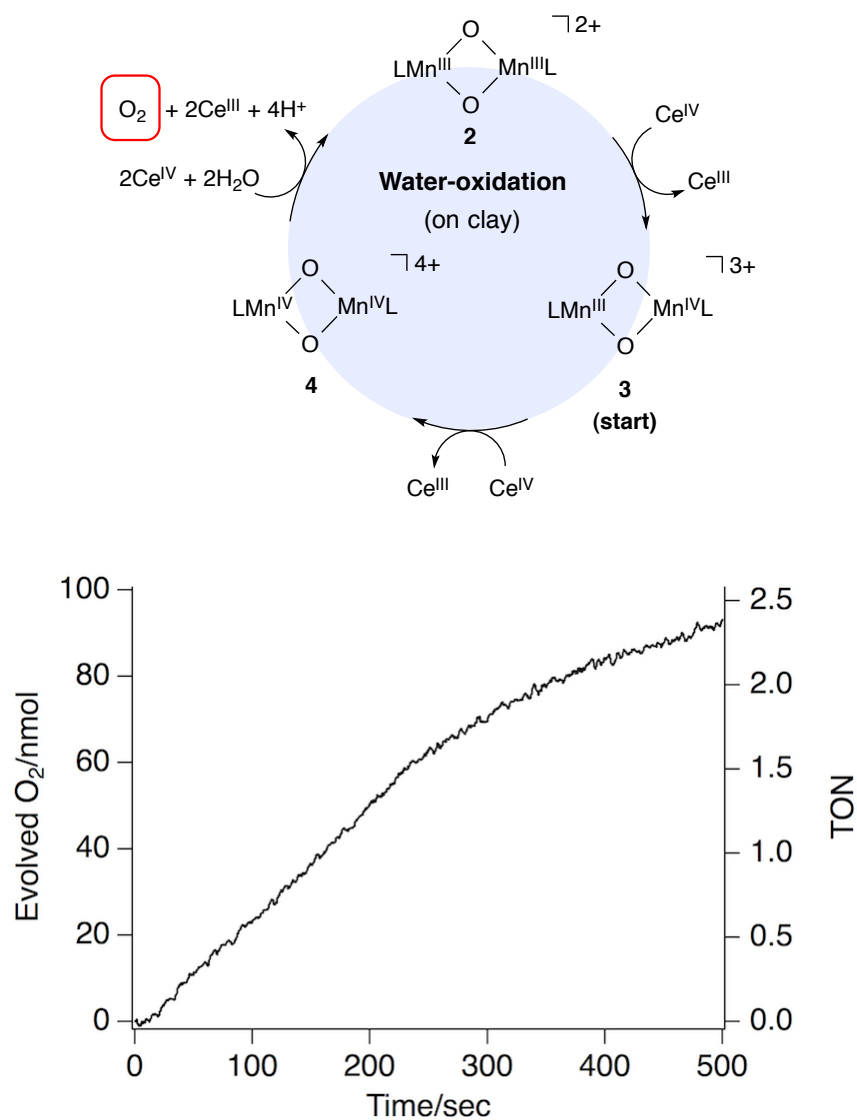


Fig. S13 Time course of the evolved O₂ from the aqueous suspension (2.0 mL) of **3@Clay** (600 μg, content of **3**: 39 nmol) with an excess amount of (NH₄)₂[Ce^{IV}(NO₃)₆] (137 mg, 250 μmol).

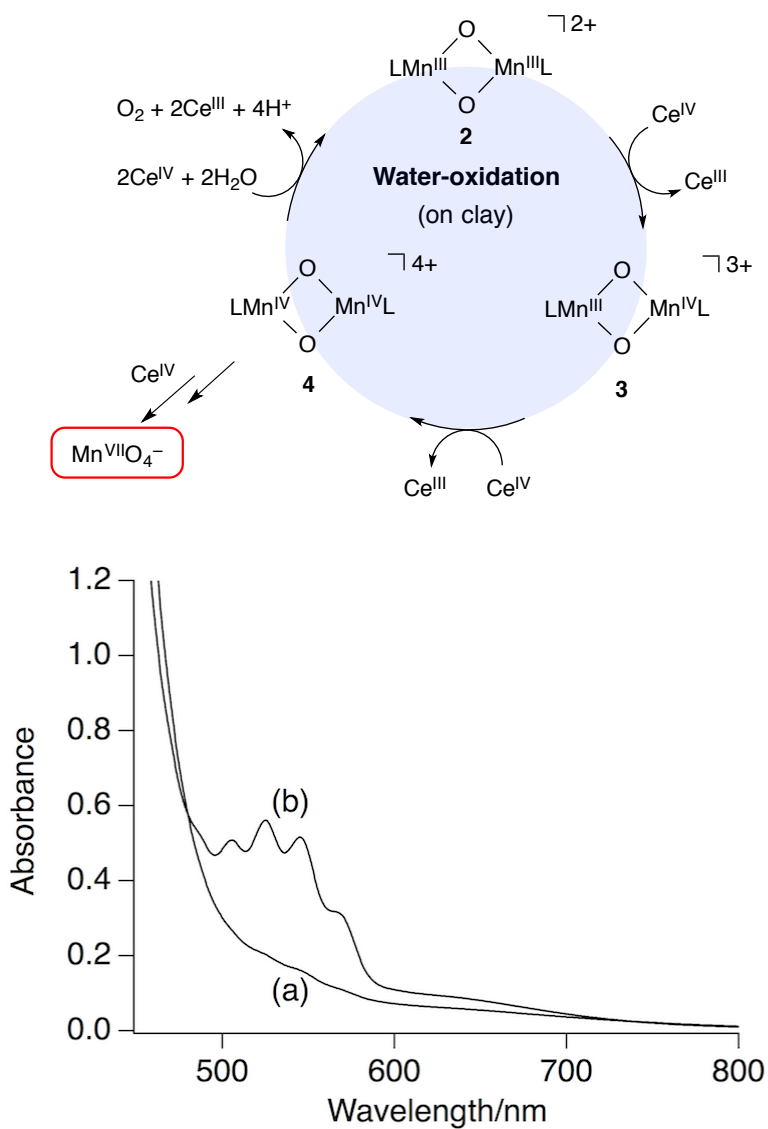


Fig. S14 UV-vis spectra of the supernatant solution (3.0 mL) of the reaction of **3@Clay** (30 mg, content of **3**: 2.0 μ mol) with an excess amount of (NH₄)₂[Ce^{IV}(NO₃)₆] (274 mg, 0.50 mmol) after (a) 0.5 min and (b) 60 min.

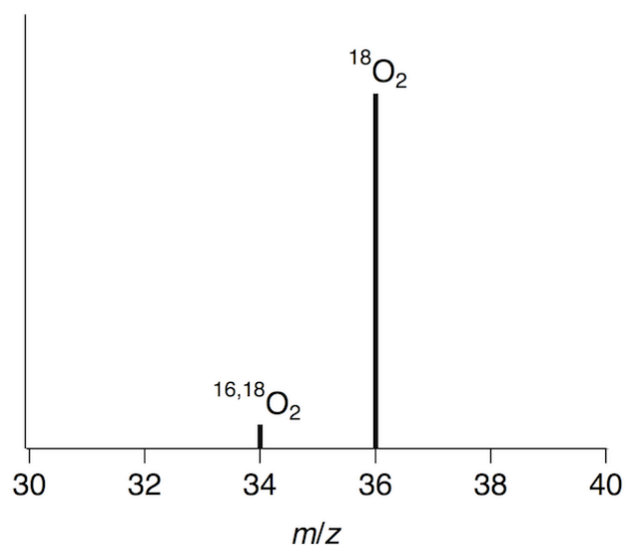
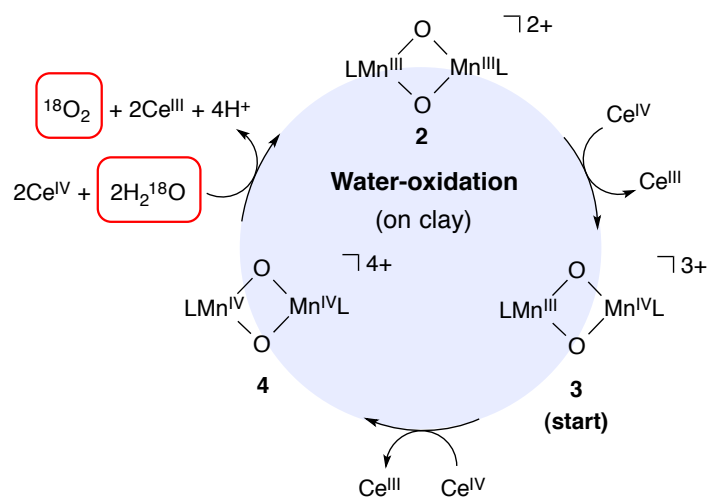


Fig. S15 Positive-ion GC mass spectrum of ^{16,18}O₂ and ¹⁸O₂ obtained from the H₂¹⁸O suspension (100 μL) of **3@Clay** (15 mg, content of **3**: 980 nmol) and (NH₄)₂[Ce^{IV}(NO₃)₆] (27 mg, 49 μmol).

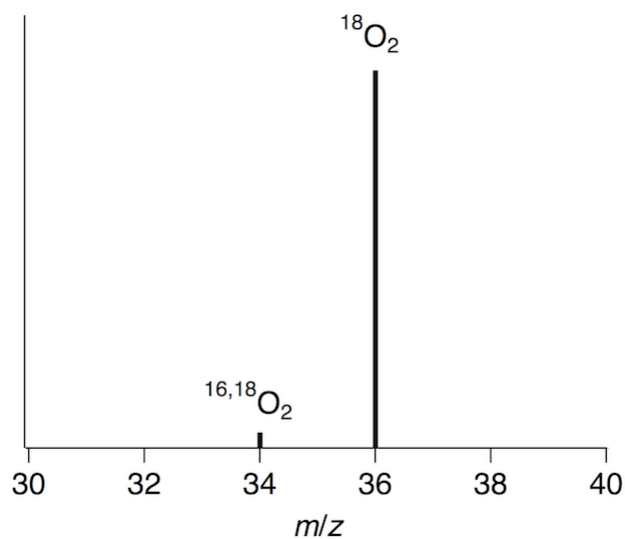
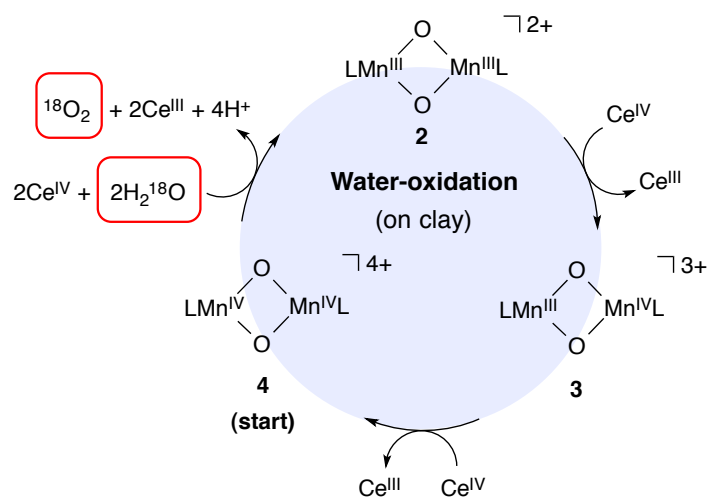


Fig. S16 Positive-ion GC mass spectrum of ^{16,18}O₂ and ¹⁸O₂ obtained from the H₂¹⁸O suspension (100 μL) of **4@Clay** (50 mg, content of **4**: 1.0 μmol) and (NH₄)₂[Ce^{IV}(NO₃)₆] (27 mg, 49 μmol).